J. Fluid Mech. (1992), *vol.* 236, *pp.* 497–511
Printed in Great Britain

Prediction of film inversion in two-phase flow in coiled tubes

By G. F. HEWITT AND S. JAYANTI
Department of Chemical Engineering and Chemical Technology, Imperial College of Science, Technology and Medicine, London SW7 2BY, UK

(Received 26 October 1990 and in revised form 26 August 1991)

Depending on the flow conditions, the liquid film in annular two-phase flow in coiled tubes may be pushed towards the outer or the inner side by the centrifugal force. It is important to understand the mechanism of this 'film inversion' in order to develop a predictive model for the film thickness distribution. In this paper, this phenomenon is studied analytically, and a new criterion, based on the secondary flow in the thin liquid film, is proposed to predict its occurrence. The criterion shows good agreement with available experimental data. It is suggested that the analytical model can readily be extended to predict the distribution of the film thickness and film flow rate in coiled tubes.

1. Introduction

Annular gas–liquid flow is a two-phase flow regime in which part of the liquid flows in the form of a thin film, and the rest of the liquid in the form of droplets entrained in the gas core. It widely occurs in many process and power generation industries, and in many practical cases it is important to know the liquid film thickness distribution. For example, the disappearance of a liquid film is associated with caustic gouging and thermal fatigue in steam generators operating at high pressures. Similarly, in the hydraulic transport of oil, the presence of a continuous liquid film is essential for corrosion inhibitors to reach all parts of the pipe. Another example (which led to the work reported in this paper) is the situation in a helical steam generator. Here, the critical heat flux condition (Hewitt 1981), and hence the limiting operating heat flux of the steam generator, can be significantly enhanced if the location of maximum heat flux does not coincide with the point of minimum film thickness. While the location of the maximum heat flux is generally known in such cases, the film thickness distribution is not, and it would be advantageous to be able to predict the film thickness in such cases.

However, the film thickness distribution is governed by several hydrodynamic factors, important among which is the phenomenon known as 'film inversion' (Banerjee, Rhodes & Scott 1967). It arises owing to the (differential) action of centrifugal force on the two phases, and can be briefly explained as follows. The centrifugal force is given by $\rho U^2/R_c$, where ρ is the density of the fluid, U is the axial velocity, and R_c is the radius of curvature of the coil, and thus depends on the density and velocity of each phase. Because of the significantly higher density of the liquid, one would expect the centrifugal force on the liquid phase to be much higher than that on the gas phase, and that it would be pushed towards the outer side of the coil as shown in figure 1 (*a*). Indeed, there is evidence (Jayanti & Berthoud 1988) that under the normal operating conditions of steam generators, the liquid film is thicker

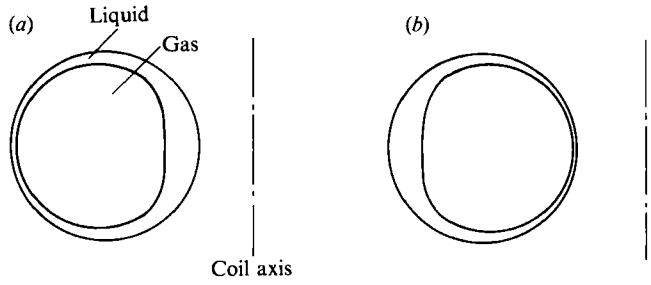

FIGURE 1. (a) Inverted, and (b) non-inverted film thickness distribution in annular two-phase flow in coiled tubes.

near the outer side. However, many low-pressure experiments (Pearce 1979; Whalley 1980) indicate that the liquid film is thicker towards the inner side of the coil (figure 1*b*). It is thought that in these cases the velocity of the gas phase is much higher than that of the liquid phase so that the centrifugal force on the former is higher in spite of the large density difference. As a result, the liquid phase is pushed into the 'inverted' position shown in figure 1(*b*). It is important to predict when and how such film inversion occurs because the hydrodynamic processes governing the film distribution (such as the entrainment of the liquid in the form of droplets) in the two cases are very different, with the serious implication that predictive models developed from results of (low pressure) laboratory experiments are not applicable for (high pressure) practical situations.

In this paper, we study this phenomenon analytically. As will be shown below, the naïve extension of the existing calculation methods for straight vertical and horizontal tubes to coiled tubes does not give meaningful results. In view of this, we start from a detailed force balance on the liquid film, and develop a new method to predict whether or not film inversion occurs for a given set of flow conditions. The study brings out the important role of secondary flow in the (very thin) liquid film in the inversion process.

2. Brief assessment of existing methods of prediction

Banerjee *et al.* (1967) studied experimentally the location of the maximum film thickness in air–water flow through coiled tubes. Their results show that the maximum film thickness is towards the inner side of the tube (i.e. in an inverted position, see figure 1) if the centrifugal force, calculated based on the average flow velocity, on the gas phase is more than that on the liquid phase. Although this criterion is very simple and appears to be physically correct, it cannot be readily applied because generally only the overall flow rate of each phase is known. Therefore, in order to apply their criterion, a method must be devised to determine the average phase velocities from given superficial velocities. The average gas-phase velocity can be taken to be approximately equal to its superficial velocity (= volumetric gas flow rate/tube cross-sectional area) because the liquid film is very thin. However, the determination of the average liquid velocity is more difficult because the film thickness, and its flow area, are not known.

There are two methods, both resulting from previous studies of two-phase flow in straight tubes for estimating the liquid phase velocity. The first is the Taitel–Dukler (1976) method of predicting the liquid height in horizontal stratified flow. The

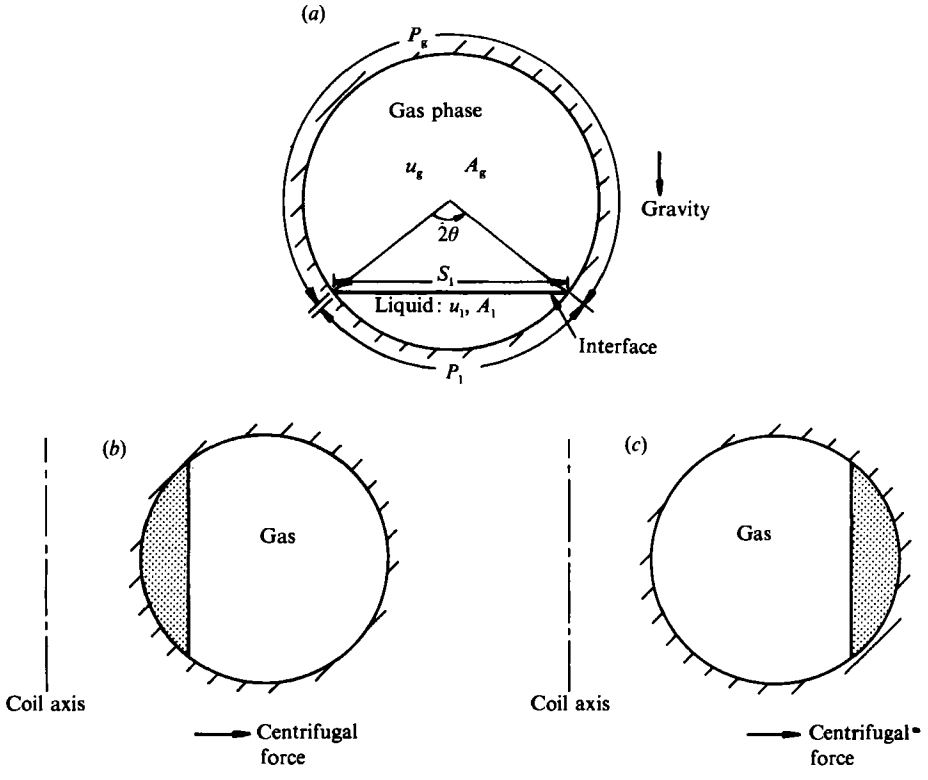

FIGURE 2. Extension of the Taitel–Dukler model (1976) to two-phase flow in coiled tubes: (*a*) for horizontal flow, (*b*) for inverted flow in coiled tubes, and (*c*) for non-inverted flow in coiled tubes.

method is based on the simplified picture of the flow system shown in figure 2(*a*). A momentum balance for fully developed flow on the gas phase gives

$$-A_g\left(\frac{dp}{dx}\right)-\tau_{wg}P_g-\tau_i S_i = 0. \tag{1}$$

Here A is the flow cross-sectional area, dp/dx is the axial pressure gradient, P is the wetted perimeter, S_i is the length of the interface and τ_w and τ_i are the shear stresses at the wall and at the interface, respectively. The subscript g refers to the gas phase. Similarly, a momentum balance on the liquid phase gives

$$-A_l\left(\frac{dp}{dx}\right)-\tau_{wl}P_l+\tau_i S_i = 0. \tag{2}$$

In this formulation, each phase is assumed to move at a constant velocity, and empirical correlations are used to calculate the shear stresses in terms of the phase velocities and friction factors. The phase velocities themselves are related to their mass flow rates through the area fractions, A_g and A_l. Thus, the equations are solved for the two unknown variables: the pressure gradient and S_i, the length of the interfacial boundary.

The method can be readily extended (neglecting gravity) to the two-phase flow in coils for the inverted and the non-inverted cases, as shown in figures 2(*b*) and 2(*c*), respectively, substituting the centrifugal force for the gravity force. However, the method was found to be very sensitive to the correlation used for the interfacial

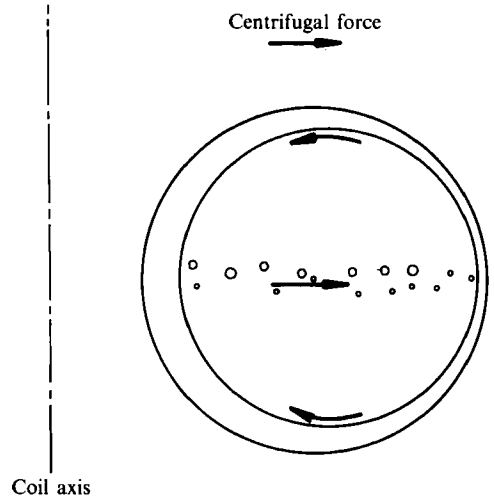

FIGURE 3. Secondary flow in the liquid film in two-phase flow through coiled tubes: the physically possible case.

friction factor, on which there is no reliable information in coils. There are other factors that render this simple model inapplicable to coiled tubes: the wall shear stress in single-phase flow varies significantly around the circumference; for example, on the outer side of the tube, it can be as much as three times its value on the inner side. This variation cannot be taken into account in the Taitel–Dukler model. Also, even for fairly significant centrifugal forces (relative to the gravitational force), the liquid film is more likely to be crescent-shaped rather than of the shape shown in figures 2(*b*) and 2(*c*), in which the case the method cannot be used.

The second method is to use the triangular relationship developed initially for vertical annular flow (Hewitt 1961; Hewitt & Hall-Taylor 1970). Here, a velocity profile, non-dimensionalized by the friction velocity, u_*(= wall shear stress/density)$^{\frac{1}{2}}$, is assumed in the liquid film; integration of this profile up to δ, the film thickness, gives the film flow rate, $\dot{m}$, in terms of δ and u_*, and thus the triangular relationship among film flow rate, film thickness and the wall shear stress. Apart from the question of its applicability for non-axisymmetric flows (Butterworth 1973; Whalley 1980; Jayanti 1990), the method has the serious shortcoming that it requires two of the three variables to be specified. It is possible to deduce the shear stress variation from the single-phase flow calculations of the type to be described later (§3.3). Although the total mass flow rate is known, this would still require specifying either the local mass flow rate variation or the film thickness variation, both of which depend on whether or not film inversion occurs, among other things. Thus, specifying either could be begging the question.

In addition to this practical difficulty in applying the criterion of Banerjee *et al.* (1967), there remains the issue of secondary flow in the liquid film. Cine films of two-phase flow in coils available at Harwell Laboratory as well as the experiments of Whalley (1980) show that there is a continuous stream of droplets from the inner side to the outer side of the coil. This can be maintained only if liquid is brought from the outer wall to the inner wall along the wall (see figure 3). The role of this secondary flow in the (usually thin) liquid film has been neglected hitherto. It is argued below that such secondary flow is possible, and that it provides a more coherent picture of the phenomenon of film inversion.

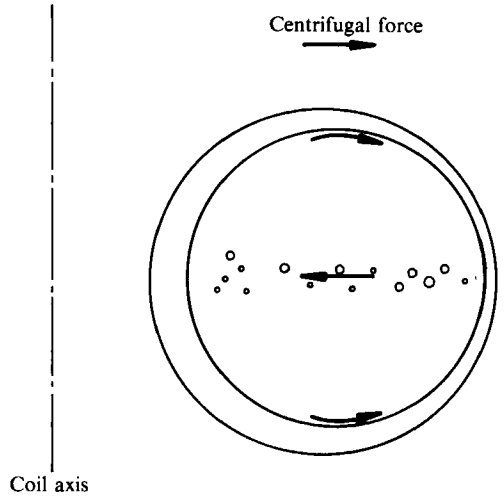

FIGURE 4. Secondary flow in the liquid film in two-phase flow through coiled tubes: the physically impossible case.

3. Mathematical model

3.1. *Outline of the argument*

The new model is based on a force balance on the liquid film in the circumferential direction. The thin liquid film flow is assumed to be laminar, and the inertial terms are neglected to give a linear axial velocity profile in the film. This is then used to evaluate the centrifugal force, and there is a force balance between the circumferential shear stress and pressure gradient created by the secondary flow in the gas phase. This gives an expression for the radial variation of the circumferential shear stress. The circumferential velocity distribution in the liquid film is then derived, thus demonstrating that there is a secondary flow in the film. It is argued that it is physically impossible to have, under steady-state conditions, a net circumferential flow in the film from the inner side to the outer side of the coil because this would require liquid droplets to travel from the outer to the inner side in the gas core in spite of the centrifugal force acting on them (see figure 4), and that a zero net circumferential flux would correspond to the film inversion point. The axial flow at this film thickness would then define the maximum liquid film flow rate that can be supported by the gas phase in an inverted position. The details of this argument are developed below.

3.2. *Details of the analysis*

In the following analysis, the effect of gravity is neglected, mainly because it does not play a major role in the film inversion phenomenon. It does have an effect on the film thickness distribution; however, this effect is negligible at high gas velocities and small coil diameters. It should be noted that such conditions are not uncommon in industrial practice (Berthoud & Jayanti 1990), and that our analysis is strictly valid under these conditions. The liquid film in two-phase flow in coiled tubes is then subjected to an axial and circumferential shear stress at the interface; a circumferential pressure gradient; and finally a centrifugal force which tends to push the liquid towards the outer side. This tendency is opposed by the circumferential shear stress and the pressure gradient created by the secondary flow in the gas phase. This is shown in figure 5. If it is assumed that the inertial terms in the (very thin)

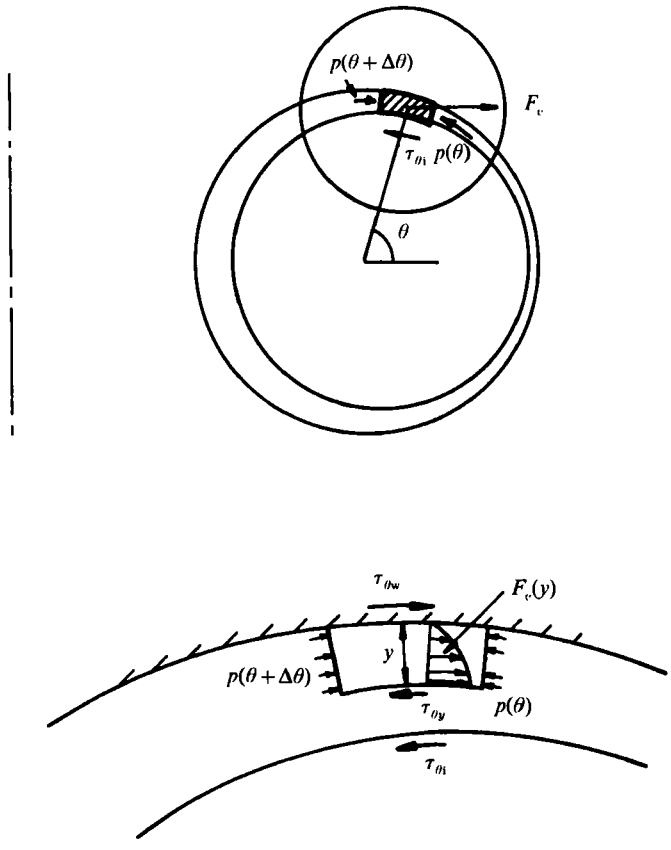

FIGURE 5. Force balance on the liquid film in annular flow in coiled tubes. F_c is the centrifugal force.

film are negligible, and that the film is laminar, then the axial momentum equation reduces to

$$\mu \frac{d^2u}{dy^2} = 0. \tag{3}$$

Here, u is the axial velocity, y is the normal distance from the wall, and μ is the dynamic viscosity of the fluid. Integrating, and imposing the shear stress boundary condition, we obtain

$$u = \frac{\tau_x}{\mu} y, \tag{4}$$

where τ_x is the axial shear stress. This expression has been obtained previously by Butterworth (1973) for annular flow in horizontal tubes.

In the circumferential direction, the situation is complicated by the presence of the centrifugal force. Again neglecting the inertial terms in the circumferential (θ-) direction, a force balance on the control volume (figure 5) gives

$$[\tau_\theta(y) - \tau_\theta(0)]\tfrac{1}{2}D\Delta\theta + [p(\theta) - p(\theta+\Delta\theta)]\,y = \left(\int_0^y \frac{\rho}{R_c} \sin\theta\, u^2\, dy\right)\tfrac{1}{2}D\Delta\theta, \tag{5}$$

where D is the tube diameter and R_c, the coil radius. Thus, the radial variation of the circumferential shear stress, $\tau_\theta(y)$, is given by

$$\tau_\theta(y) = \tau_\theta(0) - \frac{2}{D}\frac{\Delta p(\theta)}{\Delta\theta}y + \frac{\rho\tau_x^2 \sin\theta}{\mu^2 R_c}\frac{y^3}{3}. \tag{6}$$

In deriving this, (4) has been used for the axial velocity, and the pressure is assumed to be constant across the thin liquid film. In (6), the axial shear stress and the circumferential pressure gradient are imposed by the gas phase, and can be obtained from single-phase flow calculation of the flow field as discussed below. The circumferential shear stress at the wall ($y = 0$) is still unknown, but can be obtained in terms of the known circumferential shear stress at the interface, $\tau_\theta(\delta)$, and the unknown film thickness, δ, by setting $y = \delta$:

$$\tau_\theta(0) = \tau_\theta(\delta) + \frac{2}{D}\frac{\Delta\rho}{\Delta\theta}\delta - \frac{\rho\tau_x^2 \sin\theta}{\mu^2 R_c}\frac{\delta^3}{3}. \tag{7}$$

The circumferential velocity distribution, $w(y)$, can now be determined by integrating (6) for $\tau_\theta(y)$ with the boundary condition that the velocity at the wall is zero, i.e. $w(0) = 0$:

$$w(y) = \int_0^y \frac{\tau_\theta(y)}{\mu}\,\mathrm{d}y. \tag{8}$$

The net circumferential flow in the liquid film is then given by

$$\dot{m}_\theta(\theta) = \tfrac{1}{2}D\rho\,\Delta\theta\int_0^\delta w(y)\,\mathrm{d}y. \tag{9}$$

To summarize the analysis so far, we have expressed the axial and the circumferential velocities, $u(y)$ and $w(y)$, at any circumferential location θ in terms of the local film thickness, and the interfacial shear stress and circumferential pressure gradient imposed by the gas phase, both of which can be obtained by other means as shown below. Using these, we have obtained a relation between film thickness and the local net circumferential mass flux, $\dot{m}_\theta(\theta)$. We now argue that the occurrence or otherwise of film inversion can be related to the value of $\dot{m}_\theta(\theta)$.

The variable $\dot{m}_\theta(\theta)$ can take either a positive, zero or negative value. A positive value would imply a net flow from the outer side towards the inner side; this happens when the gas-imposed shear and pressure gradient overcome the centrifugal force on the liquid film. Such a net positive circumferential flow can be sustained under steady-state conditions because the loss of liquid at the outer side can be replenished by a net entrainment flux through the gas core from the inner side to the outer side as shown in figure 3. Thus, entrained drops are accelerated in the gas phase and are subjected to an increasing centrifugal force which causes them to deposit, preferentially, on the outer side of the coil. Indeed, there is experimental evidence that this happens in real cases. Whalley (1980) measured the film thickness and film flow rate around the circumference in two-phase flow through a helical coil under atmospheric conditions. The results show a sharp peaking of the axial film flow rate and film thickness on the inner side due to the inward flow along the wall in the film. However, as the gas flow rate increases, a secondary peak appears in the film thickness and film flow rate distributions near the outer side, which is presumably caused by the centrifugal force-induced redeposition of entrained liquid droplets in that region.

On the other hand, a negative value of $\dot{m}_\theta(\theta)$, which happens when the centrifugal force on the liquid is greater than the opposing gas shear and pressure force, cannot

be sustained in real cases because this would require a net entrainment flux in the gas core against the action of the centrifugal force. Thus if $\dot{m}_\theta(\theta)$ is negative, the liquid will flow along the wall from the inner to the outer side and eventually collect there, resulting in a non-inverted film (which may be spread around tube by the action of interfacial waves – this can be seen in a cine film of air–water flow through a coiled tube available at Harwell Laboratory).

Thus, a change from a negative to a positive value of $\dot{m}_\theta(\theta)$ would lead to a dramatic consequential change in the flow structure, namely, the 'inversion' of the peak in the liquid flow rate from the outside to the inside of the coil. It is interesting to consider the case when $\dot{m}_\theta(\theta)$ is zero; clearly, this case would be unstable since small negative or positive changes in the liquid flow rate would lead to stratification of the liquid to the outside or inside of the coil. However, if it were possible to maintain this condition of $\dot{m}_\theta(\theta) = 0$, then the film would be somewhat thicker on the inside owing to the circumferential variation of the axial shear stress.

We therefore conclude that film inversion occurs when $\dot{m}_\theta(\theta)$ is positive and the critical value for the film thickness, δ_c, is given by

$$\dot{m}_\theta(\theta) = \tfrac{1}{2}D\rho\,\Delta\theta\int_0^{\delta_c} w(y)\,\mathrm{d}y = 0 \tag{10}$$

at every circumferential position. This critical film thickness corresponds to a critical axial liquid flow rate (see (4)). If the actual flow rate is less than the critical value, inversion would occur; if it is greater, then film inversion would not occur, and the film would be thicker on the outer side.

3.3. *Evaluation of the interfacial shear and pressure gradient*

In order to apply the method described in §3.2, the gas-phase boundary conditions at the interface must be specified. Typical variation of the wall shear stress in the axial and the circumferential directions, and the circumferential pressure gradient in single-phase flow in coiled tubes are shown in figure 6. These were obtained from numerical calculation of the flow field in single-phase flow in coiled tubes using the HARWELL-FLOW3D computer program (Jones *et al.* 1985). The details of the calculations are described in Jayanti, Hewitt & Kightley (1990) and in more detail in Jayanti (1990). Calculations over a range of Reynolds numbers show that these curves do not change significantly. In view of this, the following simple relations were derived for the quantities required for the above method:

$$\tau_x(\theta) = \overline{\tau_x}(1.5-\theta/\pi) \quad (0<\theta<\pi), \tag{11}$$

$$\tau_\theta(\theta) = 0.12\overline{\tau_x}\sin\theta, \quad (0<\theta<\pi), \tag{12}$$

$$-\frac{\partial p}{r\,\partial\theta}(\theta) = \overline{\left(\frac{\Delta p}{r\Delta\theta}\right)}\sin\theta \quad (0<\theta<\pi), \tag{13}$$

where

$$\overline{\left(\frac{\Delta p}{r\,\Delta\theta}\right)} = \frac{p_{\text{outer}}-r_{\text{inner}}}{\frac{1}{2}D\pi} = \frac{30\overline{\tau_x}}{\frac{1}{2}\pi D}. \tag{14}$$

The above relations have been verified for a Reynolds number (based on channel diameter and mean flow velocity) between of 50000 and 200000 at a coil-to-tube diameter ratio of 26, but are expected to be approximately valid in a much wider range. Note that the mean axial shear stress ($\overline{\tau_x}$) can be estimated from a standard correlation (such as that of Ito 1959) for the friction factor in coiled tubes, and that this enables the calculation of the circumferential shear stress and pressure gradients.

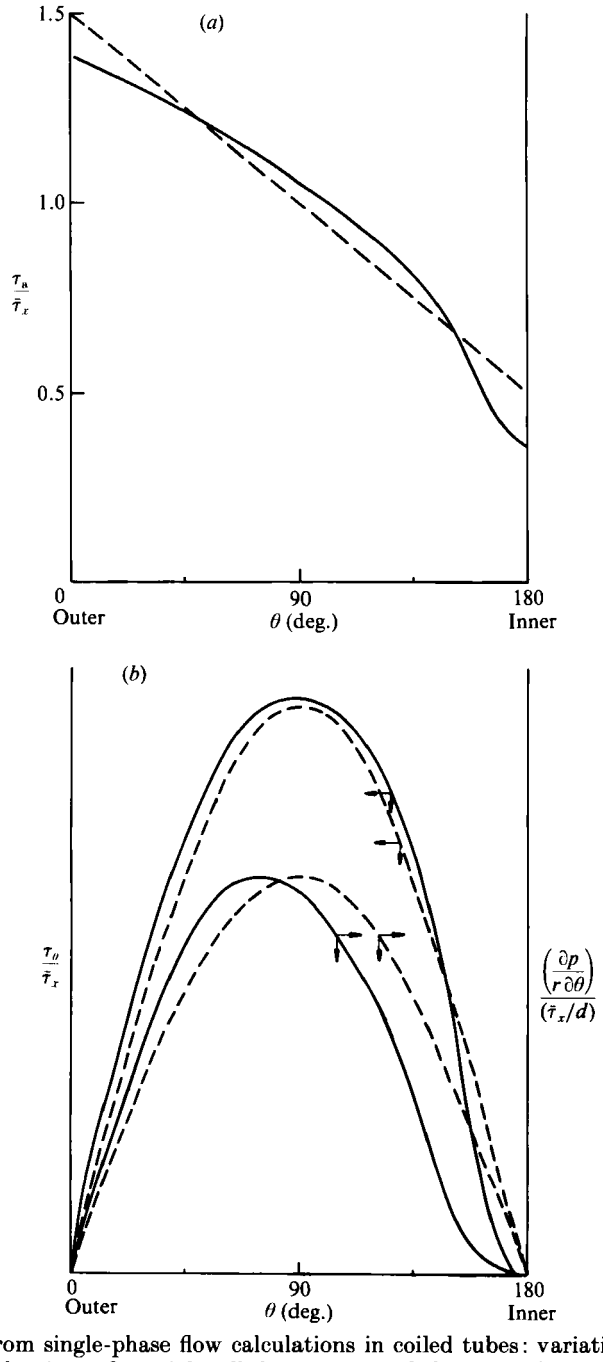

FIGURE 6. Results from single-phase flow calculations in coiled tubes: variation of (*a*) axial wall shear stress, and (*b*) the circumferential wall shear stress and the circumferential pressure gradient created in the gas phase due to secondary flow. The broken lines show the assumed distributions for each case.

The above relations were obtained from the calculation of the flow field in single-phase flow through a coiled tube, whereas in annular two-phase flow, the gas phase will be in contact with a liquid film. Although the presence of the liquid film can lead to large increases in pressure drop and axial shear stress, this effect is neglected in the

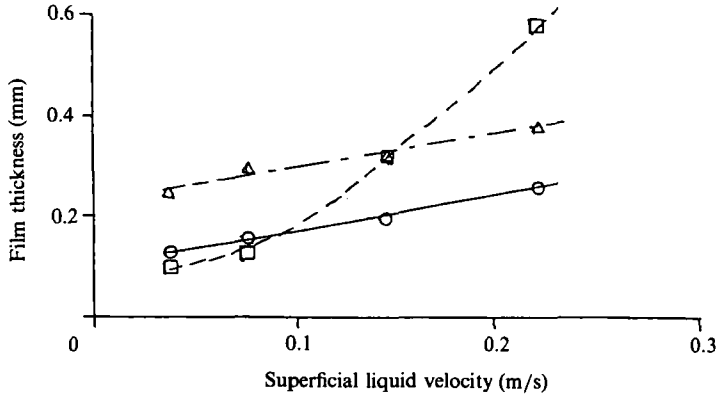

FIGURE 7. Film thickness data of Kozeki (1973): □, inner side of coil; ▽, outer side of coil; ○, straight tube.

present analysis. The justification for this is that the liquid film would be very thin over most of the tube perimeter under the conditions in which this analysis is expected to be valid, namely, high gas flow rates and small coil diameters. Also, the circumferential shear stress and pressure gradient, which are the important parameters in film inversion, and which are induced by the centrifugal force in the bulk of the gas flow, would be less affected by the presence of the liquid film.

3.4. *Calculation procedure*

It is possible to obtain an integral equation involving $\dot{m}_\theta(\theta)$ and the film thickness using (7)–(9) into which are substituted the above 'constitutive relations' (11)–(14). The simple form of (11)–(14) makes it possible to carry out the integration analytically leaving an algebraic relation between the net circumferential flow and the film thickness of the form

$$\dot{m}_\theta(\theta) = c_\tau \delta + c_{\Delta p} \delta^2 - c_{cf} \delta^5, \tag{15}$$

where the three coefficients on the right hand side of the equation represent the contribution, respectively, of the circumferential shear stress at the interface, the circumferential pressure gradient and the centrifugal force on the liquid film to circumferential flow. It should be noted that these coefficients vary circumferentially. For given coefficients, (15) is solved numerically for δ_c, the critical film thickness by setting $\dot{m}_\theta(\theta)$ equal to zero at each angular position. The critical film thickness distribution so obtained is then used (using (4)) to determine the critical axial flow rate of liquid below which film inversion occurs.

4. Verification of the criterion

The above calculation procedure for the critical flow rate for film inversion is now verified by applying it to the case investigated by Kozeki (1973). He measured the film thickness in a coiled tube (of 0.0143 m tube inner diameter and a coil diameter of 0.3 m) at the inner, outer, top and bottom parts of the tube. His data show that for an air superficial velocity of 40 m/s, the film thickness on the inner side was significantly thicker than that at the outer side at water superficial velocities of 0.037 and 0.073 m/s, but was the same at 0.145 m/s, and less at 0.21 m/s, as shown in figure 7. Thus, in his case, the transition from the inverted to the non-inverted distribution occurred at a superficial liquid velocity of between 0.073 and 0.145 m/s.

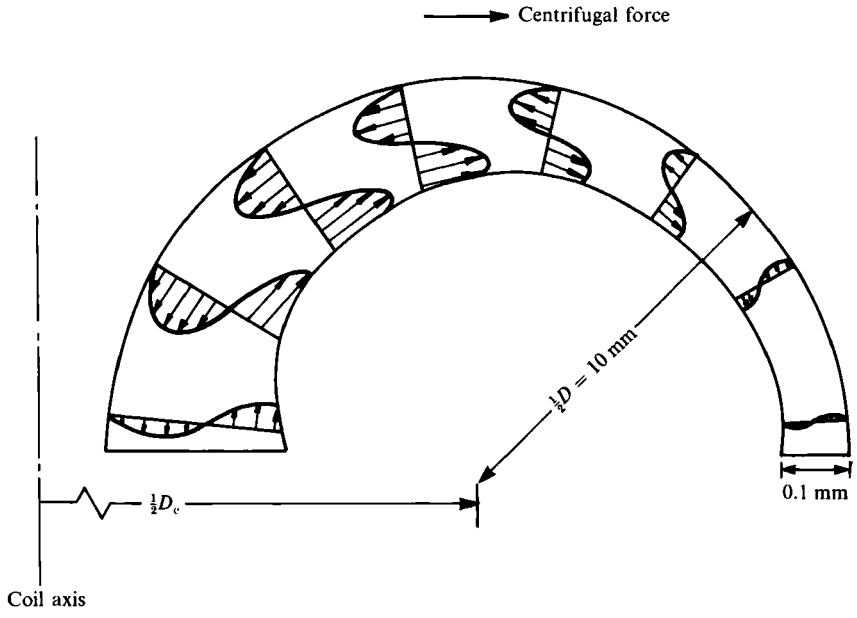

FIGURE 8. Secondary flow in the liquid film calculated from thin film analysis.

Additional supporting evidence for the criterion and the calculation method will be provided by computational fluid dynamics (CFD) calculations, and a case study of the liquid film distribution at high pressures illustrated.

4.1. *Verification using the results of Kozeki (1973)*

Equation (15) is solved at several angular positions with the conditions that $\dot{m}_\theta(\theta) = 0$ at each angular position. The coefficients in this equation are appropriate for the tube geometry and flow conditions of Kozeki's experiments. The results of the calculations are shown in figure 8 in the form of the circumferential velocity ($w(y)$) profile at various positions around the tube. A positive $w(y)$ means flow from the outer side in the inner side and vice versa. In spite of solving (15) at every circumferential position independently (i.e. without any feedback of information from neighbouring points), we find that there is an overall secondary flow in the liquid film. The fluid near the interface moves towards the outer side (against the interfacial shear) and returns along the bottom half of the film towards the inner side. This means that in the upper layer, where the axial velocity is high, the centrifugal force ($= \rho u^2/R_c$) overcomes the shear and pressure forces and pushes the liquid towards the outer side. However, in the lower part near the wall, the centrifugal force is much less because of smaller axial velocity, and the fluid is pushed towards the inner side, thus completing the secondary flow path in the liquid film.

The overall liquid film flow rate corresponding to the zero net circumferential flow case can be obtained by integrating the axial velocity profiles in the liquid film. This would correspond to the maximum liquid film flow rate that can be maintained in an inverted film (thicker on the inner side). If the flow rate is increased any further, the increased velocity, and hence the centrifugal force, will create a net circumferential flow towards the outer side which results eventually in a non-inverted film that is thicker on the outer side. Thus this film flow rate (expressed more familiarly in terms of superficial liquid velocity) corresponds to the film inversion point. The critical

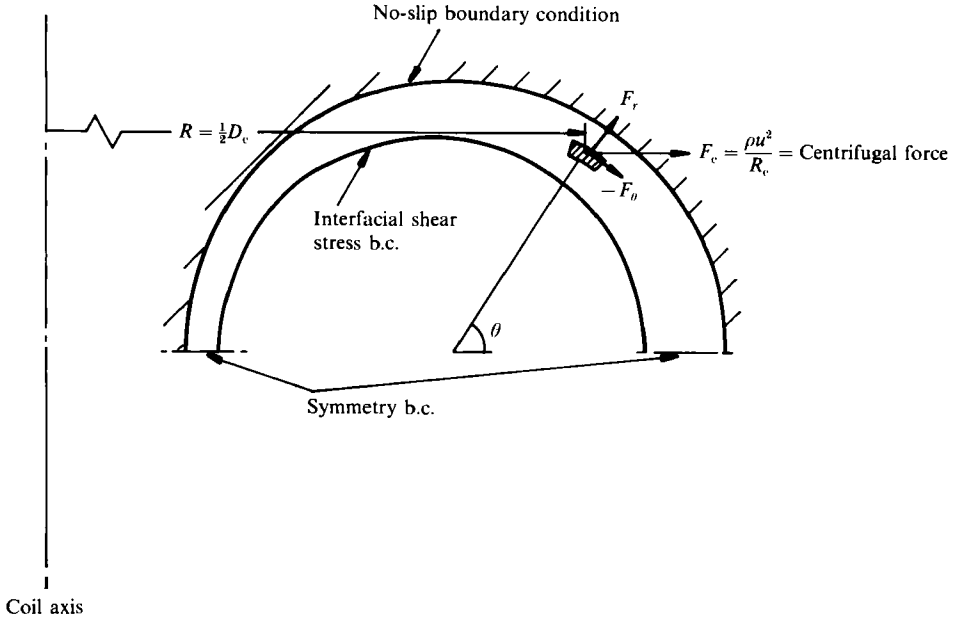

FIGURE 9. CFD simulation of the flow field in the liquid film using the straight-tube method: problem specification.

value of the superficial liquid velocity for the Kozeki case obtained from our calculations was 0.14 m/s which compares very favourably with the experimental value of between 0.073 and 0.145 m/s (Kozeki 1973).

The average liquid film velocity in this case was 1.35 m/s. Thus the ratio of the centrifugal force on the liquid phase to that on the gas phase at this critical point was 0.87. This is in good agreement with the experimental observation (Banerjee *et al.* 1967) that at the transition, the centrifugal force on the two phases is the same. This again verifies the calculation procedure.

4.2. *Confirmation of the flow field by CFD calculations*

It may appear unphysical that the liquid film at the interface should move towards the outer side in spite of the interfacial shear, as obtained in the above calculations (figure 8). In order to confirm this by other means, we have studied numerically (using CFD techniques) the behaviour of the liquid film subjected to interfacial shear and centrifugal force. The specification of the problem is summarized in figure 9. The fluid is taken to be flowing through the annular region enclosed by two cylinders, the outer one representing the tube itself and the inner one the gas core. In order to simulate the coiling effect on the liquid film, a centrifugal force field, given by $\rho u^2/R_c$, is added to the momentum equations. (This 'straight tube' approximation is shown to give accurate results if the coil-to-tube diameter ratio is greater than about ten (Jayanti *et al.* 1990).) A no-slip boundary condition is imposed on the outer (tube) wall while various (interfacial) boundary conditions are used on the inner cylinder. Since the flow is expected be symmetric about the horizontal axis in the absence of gravity, the flow through only half the tube is simulated. Symmetry boundary conditions are used on the two sidewalls. The numerical calculations were done using the HARWELL-FLOW3D computer program (Jones *et al.* 1985), and the results are described below.

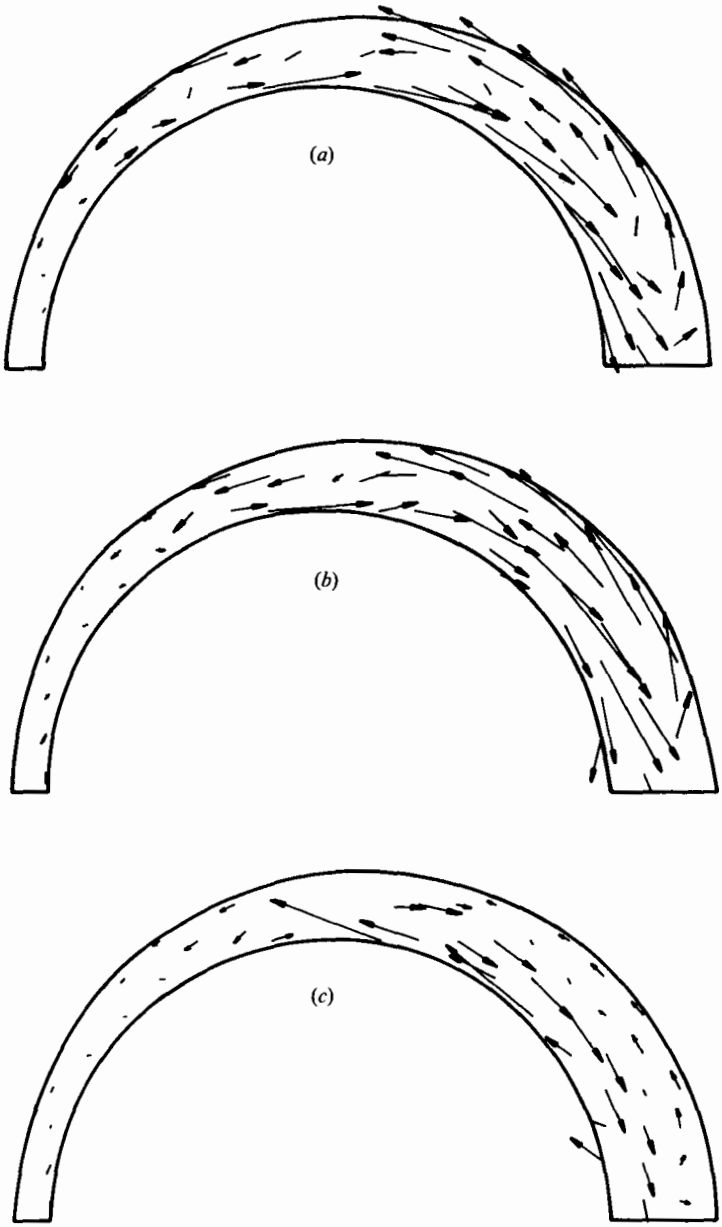

FIGURE 10. Results from CFD simulation: (*a*) for zero interfacial shear stress, (*b*) for $\tau_\theta = 0.1\overline{\tau_x} \sin\theta$ and (*c*) for $\tau_\theta = 0.5\overline{\tau_x} \sin\theta$.

When a no-shear boundary condition is used at the interface, the velocity there would be maximum, and the fluid near the interface would move to the outer side and the fluid close to the outer cylinder would move towards the inner side, thus creating a single secondary flow vortex. This is shown in figure 10(*a*).

This case is hypothetical because the gas phase in two-phase flow is expected to exert some interfacial shear; however, it serves to illustrate the effect of the centrifugal force. The real case of non-zero axial and circumferential shear stress at the interface is shown in figure 10(*b*). The magnitude of these stresses is typical of those expected to be induced by the gas phase in a coiled tube. It can be seen that

for this case (figure 10*b*), the secondary flow pattern is the same as that in figure 8: the fluid at the interface still moves towards the outer side in the direction of the centrifugal force. It is only when the circumferential shear stress at the interface is increased to very high values do we see (figure 10*c*) the fluid at the interface moving in the direction of the interfacial shear. For this case, the circumferential shear stress at the interface was about 40% of the axial shear stress. Such high values are not expected to occur in the gas phase for the diameter ratios under consideration ($D_c/D > 20$). Thus, the results of this simulation confirm the creation of secondary flow of the type shown in figure 8 in the liquid film.

4.3. *A high-pressure test case*

Although low-pressure experiments mainly show an inverted film in annular flow through coiled tubes, it appears (Berthoud & Jayanti 1990) that at high pressures, the film is non-inverted, i.e. it is thicker on the outer side. This experimental observation can be used as a further test of the criterion; its applicability can be verified by simulating a typical high-pressure steam–water flow in a coil. The geometry of the coil in this calculation is the same as that in Kozeki (1973). However, saturated steam and water properties at 98 bar are used. The steam flow rate is taken to be 500 kg/m^2 s, which at a quality of 50% corresponds to a total mass flux of 1000 kg/m^2 s, which is typical of the mass fluxes used in practical steam generators. For this set of conditions, a critical liquid superficial velocity of 0.06 m/s is obtained from the model. (The ratio of the centrifugal force on the liquid phase to that on the gas phase is a credible 0.84.) This corresponds to a critical liquid mass flux of only 45 kg/m^2 s. This means that if the liquid mass flux is greater than 45 kg/m^2 s (which is normally the case), the net circumferential flux in the liquid film would be negative and the film would become thicker on the outer side. In other words, for typical values of mass fluxes used in steam generators operating at high pressures, the liquid film would be on the outer side. This is consistent with the observations of Jayanti & Berthoud, and provides additional support for the validity of the calculation procedure described in §3.

5. Conclusion

A method based on the force balance within the liquid film is developed to determine the film inversion point. For given geometric conditions, fluid properties and gas flow rate, the method predicts the liquid superficial velocity at which the centrifugal force on the liquid film is balanced by the circumferential shear stress at the interface and the circumferential pressure gradient imposed on the liquid film by the secondary flow in the gas phase. At this point, the centrifugal force on each phase is roughly the same, which according to Banerjee *et al.* (1967) corresponds to the point of film inversion. If the actual liquid flow rate is less than this, the liquid film would be in an inverted position, i.e. thicker on the inner side of the coil.

The method also provides a mechanism – the secondary flow in the liquid film – through which the inversion occurs. For any increase in the liquid velocity beyond the critical velocity, the centrifugal force on the liquid film overcomes the shear and the pressure force imposed by the gas phase, and creates a net circumferential flow in the film towards the outer side leading eventually to a non-inverted liquid film that is thicker on the outer side.

Results of the calculations show good agreement with experimental data of Kozeki (1973) for the point of film inversion. They also provide a coherent explanation for

the discrepancy between the film thickness distributions at low and high pressures. The analysis is restricted to the cases where the effect of gravity can be neglected, i.e. for high gas flow rates and small coil diameters. However, this is not as limiting a condition as it may appear since many examples of industrial situations in which it is met can be found in Berthoud & Jayanti (1990).

REFERENCES

Banerjee, S., Rhodes, E. & Scott, D. S. 1967 Film inversion of co-current two-phase flow in helical coils. *AIChE J.* **13**, 189–191.

Berthoud, G. & Jayanti, S. 1990 Characterisation of dryout in helical coils. *Intl J. Heat Mass Transfer* **33**, 1451–1463.

Butterworth, D. 1973 An analysis of film flow for horizontal annular flow and condensation in a horizontal tube. *UKAEA Rep.* AERE R 75775.

Hewitt, G. F. 1961 Analysis of annular two-phase flow: Application of the Dukler analysis to vertical upward flow in a tube. *UKAEA Rep.* AERE R 3680.

Hewitt, G. F. 1981 Burnout. In *Two-phase Flow and Heat Transfer in the Power and Process Industries* (ed. A. E. Berlges, J. G. Collier, J. M. Delhaye, G. F. Hewitt & F. Mayinges), chap. 5. Hemisphere.

Hewitt, G. F. & Hall-Taylor, N. S. 1970 *Annular Two-phase Flow.* Pergamon.

Ito, H. 1959 Friction factors for turbulent flow in curved pipes. *Trans. ASME* D: *J. Basic Engng* **81**, 123–134.

Jayanti, S. 1990 Contribution to the study of non-axisymmetric flows. Ph.D. thesis, Imperial College, University of London.

Jayanti, S. & Berthoud, G. 1988 Dryout in helical coils. *3rd Intl Topical Meeting on Nuclear Power Plant Thermal Hydraulics and Operations, Nov. 14–17, 1988, Seoul; Paper* A2.A-4.

Jayanti, S., Hewitt, G. F. & Kightley, J. R. 1990 Fluid flow in curved ducts. *Intl J. Num. Methods Fluids* **10**, 569–589.

Jones, I. P., Kightley, J. R., Thompson, C. P. & Wilkes, N. S. 1985 FLOW3D, a computer code for the prediction of laminar and turbulent flow and heat transfer: Release 1. *UKAEA Rep.* AERE R 11825.

Kozeki, M. 1973 Film thickness and flow boiling for two-phase annular flow in helically coiled tube. *Proc. Intl Meeting on Reactor Heat Transfer, Karlsruhe, Germany*, pp. 351–372.

Pearce, D. L. 1979 Film waves in horizontal annular flow: space-time correlator experiments. *CEGB Rep.* CERL/RD/L.N 111/79.

Taitel, Y. & Dukler, A. E. 1976 A model for predicting flow regime transitions in horizontal and near horizontal gas-liquid flow. *AIChE J.* **22**, 47–55.

Whalley, P. B. 1980 Air–water two-phase flow in a helically coiled tube. *Intl J. Multiphase Flow* **6**, 345–356.